DOI: 10.1002/ejic.201000824

Distortional Isomerism in Copper(II) Nitrato Complexes of *N*,*N*′,*N*′′-Tris{[(*para*-nitrobenzyl)phenyl]aminoethyl}amine

Ann Almesåker,[a,b] Patrick Gamez,[b,c] Janet L. Scott,[a][‡] Simon J. Teat,[d] Jan Reedijk,*[b,e] and Leone Spiccia*[a]

Keywords: Copper / Tripodal ligands / Coordination modes / Hydrogen bonds / Distortional isomerism

The tris(aminoethyl)amine derivative tris{[(*para*-nitrobenzyl)phenyl]aminoethyl}amine [(*p*-NO_2BP)$_3$tren] was reacted with copper(II) nitrate in thf to yield three different solvates of [Cu(*p*-NO_2BP)$_3$trenNO_3]NO_3 (**C1**) in the solid state, namely α-**C1**·2thf (**C2**), β-**C1**·2.5thf (**C3**) and α-**C1**·(thf)$_{1.5}$·(*i*Pr_2O)$_{0.25}$ (**C4**). The light green-yellow coloured complexes, **C2** and **C4**, are different solvates of the one distortion isomer, while the dark-green **C3** is a different distortion isomer. The spectral properties of these distortion isomers were examined, and the structures of **C3** and **C4** were determined by X-ray crystallography. The difference in the physical properties (EPR and reflectance electronic spectra) of the light and dark green solids of **C1** (α-**C1**·2thf and β-**C1**·2.5thf) can be attributed to a change in the coordination mode of the ligand to the Cu^{II} centre. While the coordination sphere and orientation of the donor atoms in **C3** and **C4** are similar and the axial Cu–N and Cu–O distances identical, their equatorial bond lengths [Cu(1)–N_{eq}] differ significantly. Compound **C4** was found to have a more uniform distribution of Cu(1)–N_{eq} bond lengths [2.166(3)–2.232(3) Å] than **C3** [2.077(3)–2.352(3) Å], one Cu–N_{eq} distance being unusually long, when compared with similar bonds in a range of copper(II) complexes of tren derivatives.

Introduction

The coordination chemistry of the tripodal ligand tris(aminoethyl)amine (tren) and more elaborate structures thereof continues to be of significant interest.[1] These ligands can adopt mono-, di-, tri- or tetradentate coordination modes when reacted with a variety of metal ions, the last being the most common.[1] Ligands based on tren have often been applied in the synthesis of copper(II) complexes, and the majority of them adopt a trigonal-bipyramidal geometry in which these tripodal ligands use all four nitrogen atoms to bind to the copper(II) ion, leaving one open coordination site in the trigonal bipyramid for an exchangeable monodentate ligand.[1] This open coordination site has often been used in the stabilization of highly reactive species, such as copper–dioxygen complexes,[2,3] or the stabilization of redox-active anions, such as thiosulfates and thiosulfonates.[4]

Copper(II) is sometimes found to adopt different geometries with the same ligand due to the "plasticity" of the copper(II) ion.[5,6] Distortion isomers have been reported, which have distinctly different colours arising from only slight distortions in the coordination sphere of the copper(II) ion,[6,7] and, in some cases, distortion isomers have been isolated as differently solvated species.[8]

We recently reported that the [Cu(*p*-NO_2BP)$_3$trenF]BF_4 complex can be formed by reaction of a tren-based ligand, (*p*-NO_2BP)$_3$tren, with Cu$(BF_4)_2$·$6H_2O$. The fluoride ligand can be generated from the hydrolysis of a BF_4^- anion or introduced by the addition of a fluoride salt. Analysis of the structure of this compound revealed the shortest ever reported Cu^{II}–F distance, indicating very strong binding of fluoride to the Cu^{II} centre.[9] The bulky *para*-nitrobenzylphenyl *N*-substituents on (*p*-NO_2BP)$_3$tren were found to create a tight hydrophobic cavity that prevented the fluoride ion from forming bridged complexes and from accepting hydrogen bonds from hydrophilic molecules. This finding led us to postulate that the presence of bulky *N*-substituents on the tren moiety could be exploited in the synthesis of further complexes with interesting crystallographic features

[a] School of Chemistry and Centre for Green Chemistry, Monash University,
Victoria 3800, Australia
Fax: +61-3-9905-4597
E-mail: leone.spiccia@monash.edu
[b] Leiden Institute of Chemistry, Gorlaeus Laboratories, Leiden University,
P. O. Box 9502, 2300 RA Leiden, The Netherlands
Fax: +31-71-527-4671
E-mail: reedijk@chem.leidenuniv.nl
[c] ICREA, Universitat de Barcelona, Departament de Química Inorgànica,
Diagonal 647, 08028 Barcelona, Spain
[d] Advanced Light Source, Lawrence Berkeley National Laboratory,
Berkeley, California 94720, USA
[e] Department of Chemistry, King Saud University,
P. O. Box 2455, Riyadh 11451, Saudi Arabia
[‡] Current address: Centre for Sustainable Chemical Technologies, University of Bath,
Bath, BA2 7AY, UK

and physical properties. We report herein the isolation of different solvated species and distortion isomers from the reaction of $(p\text{-}NO_2BP)_3$tren with $Cu(NO_3)_2{\cdot}3H_2O$ in thf, and their characterization by X-ray crystallography, EPR spectroscopy and UV/Vis/NIR spectrophotometry.

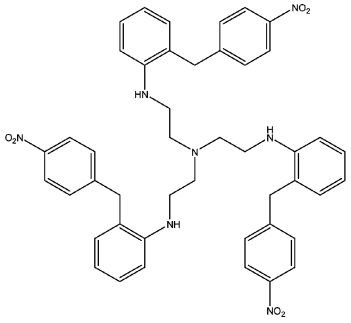

$(p\text{-}NO_2BP)_3$tren

Results and Discussion

Synthesis

Reaction of $(p\text{-}NO_2BP)_3$tren with $Cu(NO_3)_2{\cdot}3H_2O$ in thf resulted in the instant formation of a green solution of **C1**, $[Cu(p\text{-}NO_2BP)_3trenNO_3](NO_3)$. Slow diffusion of diethyl ether into this solution resulted in the crystallization of two distinctively different coloured solids, **C2** (green-yellow, α-**C1**) and **C3** (dark green, β-**C1**), shown in Figure 1. Initially, dark and light coloured solids formed as mixtures, or in an unpredictable manner. Controlling the temperature of crystallization allowed the selective crystallization of one compound over the other (Scheme 1). Vapour diffusion of diethyl ether at room temperature or above (≥25 °C) yielded the light green-yellow **C2** exclusively, while the darker **C3** (β-**C1**) was isolated from vapour diffusion in a cold room (5 °C) or in the freezer (–20 °C). A slight excess of the copper(II) nitrate also aided in the formation of the darker **C3**. When diethyl ether was replaced by diisopropyl ether at room temperature, to slow the crystallization process, **C4** formed instead of **C2**. **C4** has the same spectral properties as **C2**, and the complex in **C4** was hence assigned to have the same conformation as in **C2**, that is, the same distortion isomer (α-**C1**), with a slight change in the content of lattice solvent.

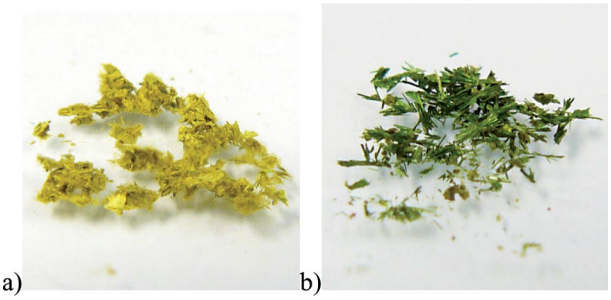

Figure 1. The two differently coloured complexes: (a) light yellow-green **C2** and (b) dark green **C3**.

Solution Studies

Although three different solvates (two distortion isomers) could be formed in the solid state, only one compound could be detected in solution, namely **C1**. The electronic spectrum of a green solution of the complex in thf exhibited a major band at λ_{max} = 685 nm (ε_{max} = 270 $M^{-1}cm^{-1}$) and a less intense shoulder at λ = 605 nm (Figure 2a) consistent with the formation of a distorted trigonal-bipyramidal copper(II) complex.[10] The EPR spec-

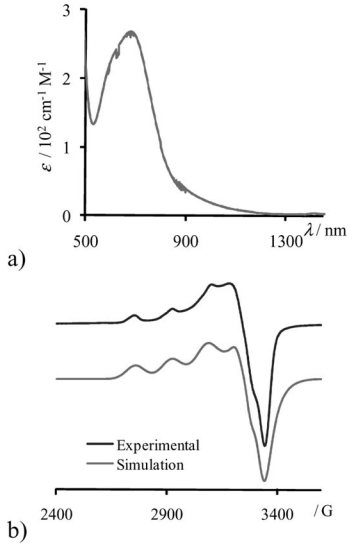

Figure 2. (a) UV/Vis/NIR spectrum of a thf solution of **C1** formed in situ. (b) EPR spectrum (dark grey) of a frozen thf solution of **C1** formed in situ (77 K) and the simulated spectrum (light grey). Simulated values: g_x = 2.012, g_y = 2.045, g_z = 2.182 and A_x = 1.8, A_y = 4.2, A_z = 16.4 mT.

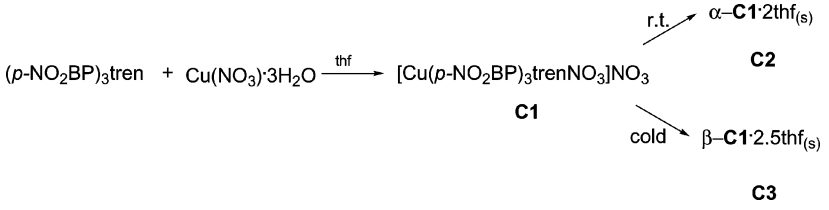

Scheme 1. Temperature-controlled formation of **C2** and **C3** by vapour diffusion of diethyl ether into a thf solution of **C1**.

trum of the same solution showed a signal typical for a copper(II) ion in a distorted geometry with a $d_{x^2-y^2}$ ground state (g_x = 2.012, g_y = 2.045 and g_z = 2.182, Figure 2b), which is generally found for copper(II) in a square-pyramidal geometry.[11] It should be noted, however, that similar parameters have also been reported for trigonal-bipyramidal copper(II) complexes exhibiting only small distortions towards a square-pyramidal environment, including some complexes of tripodal tren ligands.[12]

Solid-State Studies

C2 and **C3** were examined by their electronic reflectance, IR and EPR spectra. The spectroscopic data for the two solids were found identical, apart from slightly shifted spectral features. This indicates that, despite the clear colour difference, almost identical complexes had formed, as distortion isomers. The observed electronic reflectance spectra of the two compounds, with a maximum at around 900 nm and a shoulder around 700 nm, appeared to be significantly shifted from the solution spectrum and have characteristics more typical of trigonal-bipyramidal copper(II) complexes.[10] The solid-state EPR spectra of the two compounds consist of essentially the same isotropic or close to isotropic signals with *g* values around 2.1. No improvement in the resolution of the signals was seen at 77 K relative to those recorded at room temperature (Figure 3).

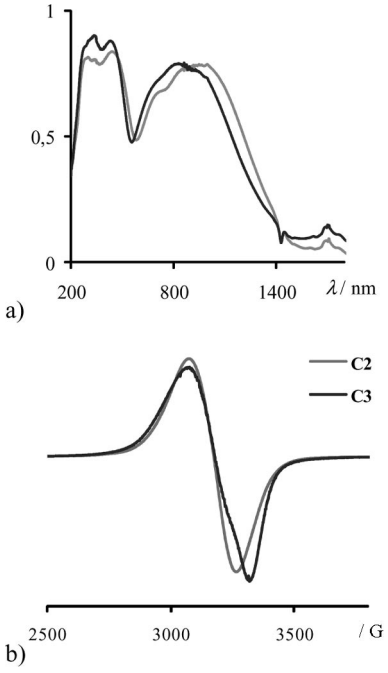

Figure 3. (a) Room-temperature reflectance electronic spectra and (b) EPR spectra recorded at 77 K for **C2** (light grey lines) and **C3** (dark grey lines).

The IR spectra of the two solids also show only subtle differences. The N–H stretches, which were observed at 3390 cm^{-1} for the parent ligand, were found at 3241 and 3212 cm^{-1} in the spectrum of **C2** and **C3**, respectively. The typically distinguishable asymmetric NO_2 stretching vibrations of the nitrate ion were masked by the vibrations of the aromatic nitro groups of the ligand. Nevertheless, the presence of these vibration bands could be inferred from a broadening of the bands around 1500 cm^{-1} in the spectra of both compounds. The symmetric NO_2 stretching vibrations of the nitrate ions were more easily identified, existing as a single peak at 1282 cm^{-1} for both compounds. The bands corresponding to the aromatic and aliphatic C–H stretches, around 2900 cm^{-1}, were noticeably shifted in the complexes relative to the corresponding values for the parent ligand, although no obvious differences were observed between the two coloured crystalline solids.

Crystal Structures

Thin needle-like single crystals of **C3**, ([Cu(*p*-NO_2BP)$_3$-trenNO_3](NO_3)·2thf), obtained by vapour diffusion of diethyl ether into a thf solution of **C1** at 5 °C, were of good enough quality to allow the determination of crystal structure by using a synchrotron source. Fine, light-coloured needles of **C2** ([Cu(*p*-NO_2BP)$_3$trenNO_3](NO_3)·2.5thf) of low quality were grown at room temperature by vapour diffusion of diethyl ether. Better quality single crystals (of **C4**) were obtained by slow vapour diffusion of diisopropyl ether. The X-ray analysis revealed the presence of entrapped diisopropyl ether molecules in the lattice, that is, [Cu(*p*-NO_2BP)$_3$trenNO_3](NO_3)·1.5thf·0.25*i*Pr_2O. Compound **C4** is postulated to be a different solvate of distortion isomer **C2** (α-**C1**), in which some of the thf molecules in the lattice have been replaced by diisopropyl ether molecules.

The ORTEP diagrams of **C4** and **C3** are shown in Figure 4. Compounds **C4** and **C3** crystallized in the space groups $P2_1/c$ and $P2_1/n$, respectively, in the monoclinic crystal system. The solvent molecules in both structures were found to be highly disordered. In **C4**, two areas were occupied by solvent in the cell unit. One position was best modelled as one thf molecule disordered over two positions each with SOF (site occupancy factor) of 0.5. The second area was modelled as a thf or a diisopropyl ether molecule with SOF of 0.5 or 0.25, respectively. In **C3**, the 2.5 molecules of thf were modelled over four positions with SOF of 1, 0.5, 0.75 and 0.25.

As may have been anticipated from the spectroscopic data, analysis of the crystal structures revealed that the two complexes were similar, with some disparities in the packing of the complex cations and in the geometry around the Cu^{II} centre (see Table 1 for selected bond lengths and angles). Both structures have a five-coordinate copper(II) ion with distorted trigonal-bipyramidal characteristics (τ[13] = 0.79 and 0.70 for **C4** and **C3**, respectively).

The axial bond lengths in both **C3** and **C4** were found to be identical, within experimental error, [$d_{Cu(1)-O(11)}$ = 1.938(2) and 1.935(3) Å and $d_{Cu(1)-N(1)}$ = 2.009(2) and 2.015(3) Å]. In contrast, the equatorial bond lengths [Cu(1)–N_{eq}] differed significantly. Compound **C4** has a more uniform distribution of the Cu(1)–N_{eq} bond lengths

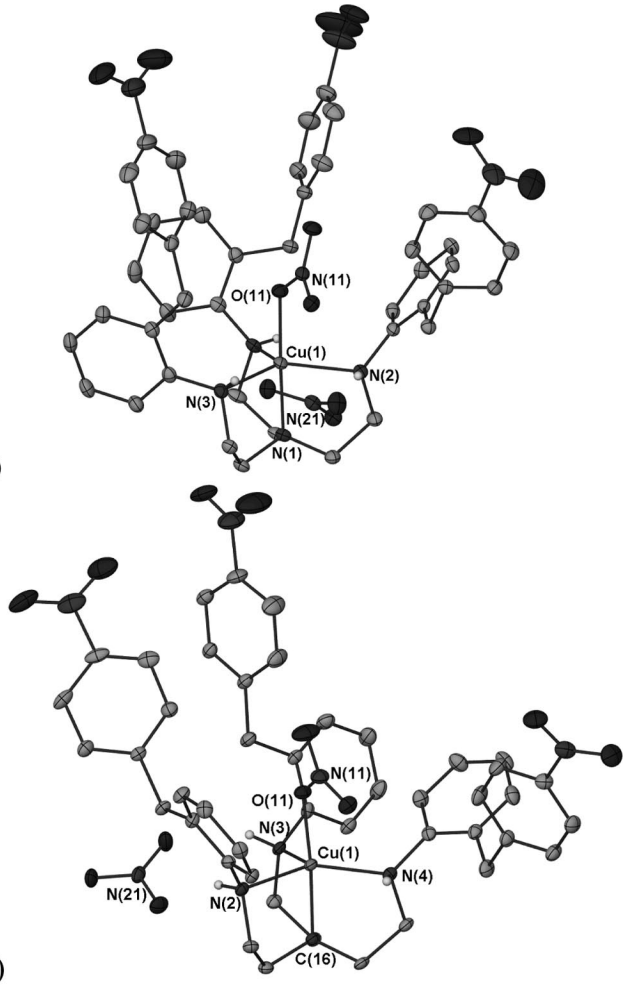

Figure 4. ORTEP diagrams showing: (a) α-**C1** of **C4** and (b) β-**C1** of **C3**. All atoms except hydrogen atoms are shown as thermal ellipsoids at the 35% probability level. Solvent molecules in the lattice and all hydrogen atoms except those belonging to the amine groups have been omitted for clarity. The benzyl section of arm N(2) in **C2** (b) was found to be disordered and best modelled over two positions (0.25:0.75 occupancy) of which only the higher occupancy position is shown.

[ranging from 2.166(3) to 2.232(3) Å], contrary to **C3**, which exhibits a greater variation [ranging from 2.077(3) to 2.352(3) Å]. This difference in Cu–N equatorial bond lengths is proposed to be responsible for the observed differences in physical and spectroscopic properties of **C3** and **C4**. In fact, the longest Cu–N_{eq} distance in **C3** is more than 0.12 Å longer than the longest Cu–N_{eq} distance in a variety of copper(II) complexes of *N*-functionalized tren derivatives (Table 2).

The three equatorial positions of the copper(II) centre are occupied by the secondary tren nitrogen atoms, N_{eq} [N(2)–N(4)], and the axial positions by the tertiary tren nitrogen atom, N_{ax} [N(1)], and one oxygen atom, O(11), from a monodentate coordinated nitrate ion ligand.[14] As often found for Cu^{II} complexes of tren ligands, the copper(II) centre is displaced out of the plane defined by the three equatorial nitrogen atoms towards the oxygen atom, O(11), by 0.188(2) and 0.204(2) Å for **C4** and **C3**, respectively, and

Table 1. Selected bond lengths (in Å) and angles (in degrees) for **C4** and **C3** (esd in parentheses).

	C4	**C3**
Bond lengths /Å		
Cu(1)–N(1)	2.009(2)	2.015(3)
Cu(1)–N(2)	2.166(3)	2.149(3)
Cu(1)–N(3)	2.232(3)	2.352(3)
Cu(1)–N(4)	2.178(3)	2.077(3)
Cu(1)–O(11)	1.938(2)	1.935(3)
Cu(1)–O(13)	2.941(3)	2.965(3)
Angles /°		
N(1)–Cu(1)–N(2)	84.9(1)	85.0(1)
N(1)–Cu(1)–N(3)	84.8(1)	82.5(1)
N(1)–Cu(1)–N(4)	85.6(1)	85.9(1)
N(1)–Cu(1)–O(11)	172.1(1)	174.1(1)
N(2)–Cu(1)–N(3)	124.4(1)	103.1(1)
N(2)–Cu(1)–N(4)	119.0(1)	132.2(2)
N(2)–Cu(1)–O(11)	94.9(1)	93.2(1)
N(3)–Cu(1)–N(4)	114.3(1)	122.0(1)
N(3)–Cu(1)–O(11)	101.7(1)	92.5(1)
N(4)–Cu(1)–O(11)	87.70(1)	99.4(1)

Table 2. Bond lengths (in Å) and τ[13] values for copper(II) complexes of tren-based ligands.

Complex	τ	$d_{Cu–Neq}$ /Å	Avg. $d_{Cu–Neq}$ /Å	$d_{Cu–Nax}$ /Å
[CutrenCl]Cl[19]	0.90	2.099(3) 2.107(3) 2.066(3)	2.091(5)	2.081(3)
[$CuMe_3$tren(CH_3CN)]-$(ClO_4)_2$[15]	0.92	2.080(2) 2.093(2) 2.111(3)	2.095(4)	2.030(2)
[Cu(2-NO_2Bz)$_3$trenCl]-Cl(EtOH)[3]	0.81	2.081(4) 2.105(4) 2.107(4)	2.098(7)	2.038(4)
[$CuBz_3$trenCl]-$ClO_4(CH_2Cl_2)(H_2O)_{0.25}$[16]	0.85	2.109(5) 2.127(5) 2.160(4)	2.132(8)	2.026(4)
[$CuGlu_3$trenCl]Cl[20]	0.99	2.125(4) 2.146(4) 2.142(4)	2.138(7)	2.008(3)
[$CuMe_3Bz_3$trenCl]-$ClO_4(CH_2Cl_2)_{1.5}(H_2O)_{0.5}$[16]	0.98	2.183(3) 2.165(2) 2.193(3)	2.180(5)	2.029(3)
[$CuMe_6$trenCl]ClO_4[21]	1.01	2.186(2) 2.186(2) 2.186(2)	2.186(3)	2.040(6)
[Cu(*p*-NO_2BP)$_3$trenF]-BF_4(thf)[9]	0.99	2.207(2) 2.160(2) 2.176(2)	2.181(3)	2.001(2)
α-**C1**·1.5thf·0.25*i*Pr_2O (**C4**)	0.79	2.166(3) 2.232(3) 2.178(3)	2.192(5)	2.009(2)
β-**C1**·2.5thf (**C3**)	0.70	2.149(3) 2.352(3) 2.077(3)	2.193(5)	2.015(3)

the Cu–N_{ax} bond lengths are shorter than the Cu–N_{eq} bond lengths.[15–17] The general trend for the Cu–N bond lengths in copper(II) tren-based complexes is that the Cu–N_{eq} distance increases as the steric bulk of the *N*-substituent increases (as has been shown in the series tren < Me_3tren ≈ Bz_3tren < Me_3Bz_3tren ≈ Me_6tren, see Table 2), while the

variation of the Cu–N_{ax} distance is minor.[15,16] As observed in our earlier work, (p-NO_2BP)$_3$tren would fit last in the series, giving the sequence tren < Me_3tren ≈ Bz_3tren < Me_3Bz_3tren ≈ Me_6tren ≈ (p-NO_2BP)$_3$tren.[9] The increase in Cu–N bond lengths upon going across the series could further be explained by the donor ability of the nitrogen atoms. Compared to secondary or primary amines, bulky tertiary amines can be poor sigma donors, weakening the coordination interaction and thus leading to longer Cu–N_{eq} bonds.[18] In the case of (p-NO_2BP)$_3$tren, the binding ability of the equatorial nitrogen atoms is affected by the attached bulky, electron-deficient aromatic rings, causing changes in bond lengths and bond angle distortion.

The particular orientation of the coordinated nitrate ion with respect to the Cu(1)–N_{ax} bond in both structures allows contact between the oxygen atom O(13) of the nitrate ion and the Cu^{II} centre. However, the Cu(1)–O(13) distances [2.941(3) and 2.965(3) Å in **C4** and **C3**, respectively] are too long to consider the corresponding bonds as real coordination bonds, namely, these distances are longer than the sum of the van der Waals radii [$r_{vdW(O+Cu)}$ = 2.92 Å].[22] The nitrate ions can be considered as monodentate in both cases.

The crystal lattice of **C4** and **C3** is stabilized by hydrogen-bonding interactions between the noncoordinating nitrate ion and the secondary amine groups of the ligand (Figure 5 and Table 3). In both cases, the nitrate ion accepts hydrogen bonds from three amine hydrogen atoms, that is, H(2N)···O(22), H(3N)···O(21) and H(4N)′···O(23).[23] In **C4**, the angle between the nitrate ion and H(2N) and H(3N) gives rise to one short and one long hydrogen bond [2.28(4) and 2.11(4) Å], and to a relatively long O(22)···H(4N)′ contact [2.55(4) Å] (Table 3). In **C3**, the corresponding distances to H(2N) and H(3N) are comparable [2.15(4) and 2.18(5) Å], and the hydrogen bond from H(4N)′ is relatively short [H···A distance 2.23(4) Å]. These H···O distances are all significantly shorter than the sum of the van der Waals radii [$d_{vdW(H+O)}$ = 2.75 Å],[22] and all six contacts can be considered to be moderate hydrogen bonds. The difference in the way the noncoordinated nitrate ion is hydrogen-bonded in the two structures was not considered to be responsible for the differences in colour or spectroscopic properties of compounds, but rather to provide stabilization of the lattices.

Table 3. Hydrogen bonds in **C4** and **C3**.

D–H···A	$d_{D–H}$ /Å	$d_{H···A}$ /Å	$d_{D···A}$ /Å	Angle$_{DHA}$ /°
C4				
N(2)–H(2N)···O(23)	0.73(4)	2.28(4)	2.968(4)	156(4)
N(3)–H(3N)···O(21)	0.84(4)	2.11(4)	2.901(4)	155(4)
N(4)–H(4N)···O(22)[a]	0.75(4)	2.55(4)	3.237(4)	154(3)
C3				
N(2)–H(2N)···O(22)	0.83(4)	2.15(4)	2.938(5)	158(4)
N(3)–H(3N)···O(21)	0.85(5)	2.18(5)	2.925(5)	146(4)
N(4)–H(4N)···O(23)[b]	0.77(4)	2.23(4)	2.957(5)	160(4)

[a] Symmetry operations: x, 1 + y, z. [b] Symmetry operations: x – 0.5, 0.5 – y, z – 0.5.

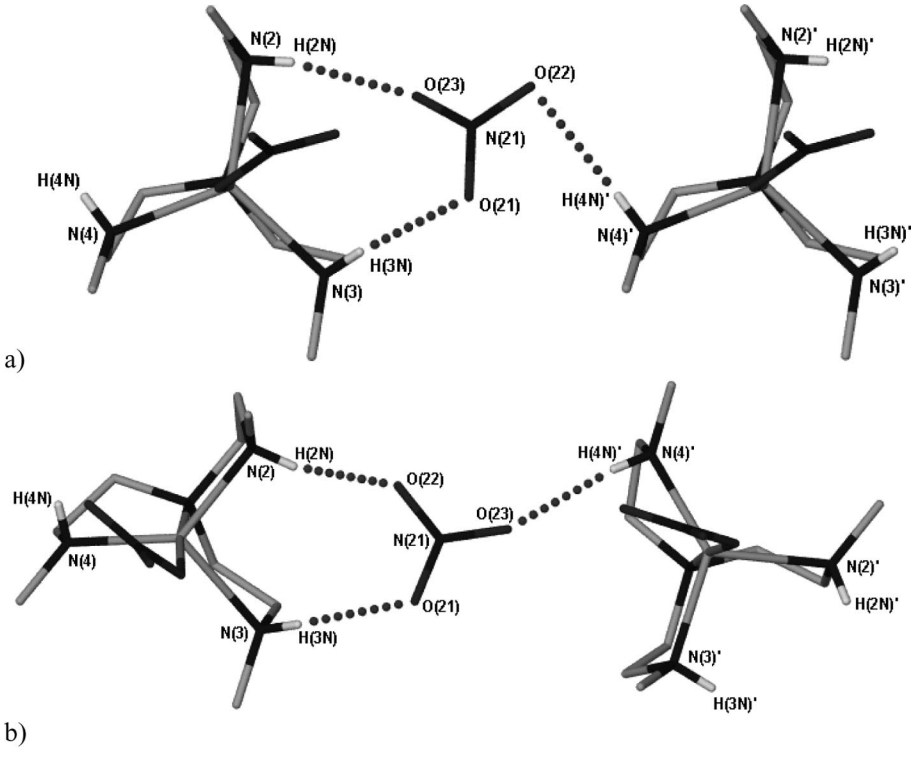

Figure 5. Schematics showing the hydrogen-bonded nitrate ion in (a) **C4** and (b) **C3**.

Conclusions

The differences in physical properties (IR, EPR and reflectance electronic spectra) between the light and dark green solids of **C1** (α-**C1**·2thf and β-**C1**·2.5thf) can be attributed to slight changes in the mode of coordination of the ligand to the Cu^{II} centre, as detected by examination of the single-crystal X-ray structures of the yellow-green **C4** and the dark green **C3**. In these compounds, the coordination sphere and orientation of the donor atoms are similar, but the bond lengths provide some indication of the origin of the different colour of the solvates. Even though the axial bond lengths are practically identical (within experimental error), the equatorial bond lengths [Cu(1)–N_{eq}] differ significantly, compound **C4** having a more uniform distribution of the Cu(1)–N_{eq} bond lengths than **C3**. Comparison of a series of Cu–tren based structures reveals that one Cu–N_{eq} bond length in **C3** is unusually long [2.352(3) Å] relative to Cu–N_{eq} distances of 2.07–2.23 Å for the related compounds. This major difference in equatorial bond length is proposed to be the cause of the physical differences between the light (**C4**) and dark (**C3**) distortion isomers of the complex.[6,7,25] These compounds highlight the well-known plasticity of the copper(II) ion.[5,6,24]

Experimental Section

General: All solvents and reagents were obtained from commercial sources and used as received. The synthesis of the ligand (*p*-NO_2BP)$_3$tren has been reported elsewhere.[26] All manipulations were carried out in air. X-band EPR spectra were recorded with a Bruker EMX electron spin resonance spectrometer. EPR spectra were simulated by using ref.[27] Solution UV/Vis/NIR spectra were measured with a Varian Cary 50 spectrophotometer (path length 1 cm), and diffuse reflectance spectra of solid samples were recorded with a Perkin–Elmer 330 spectrometer equipped with a data station. FTIR spectra were obtained with a Perkin–Elmer Paragon 1000 FTIR spectrophotometer equipped with a Golden Gate ATR device, using the reflectance technique (4000–300 cm^{-1}, resolution 4 cm^{-1}). C, H, N determinations were performed with a Perkin–Elmer 2400 Series II analyzer.

α-[Cu(*p*-NO_2BP)$_3$trenNO_3]NO_3·(thf)$_2$ (C2): A thf solution of (*p*-NO_2BP)$_3$tren (78.0 mg, 0.10 mmol, 2.5 mL) was added to a thf solution of $Cu(NO_3)_2$·$3H_2O$ (24.2 mg, 0.10 mmol, 2.5 mL). Diffusion of diethyl ether at ambient temperature overnight yielded yellow-green needles. The crystals were filtered, washed with diethyl ether and air-dried to give **C2** (85.2 mg, 76%). IR: $\tilde{\nu}$ = 3241 (w), 2860 (w br), 1598 (m), 1515 (s), 1495 (m), 1346 (s), 1282 (s) cm^{-1}. λ_{max}: 295, 335, 430, 710, 950 nm. UV/Vis/NIR (thf): λ_{max} (ε_{max}, $M^{-1}cm^{-1}$) = 400 (2940), 605 (230), 685 (270) nm. EPR (solid, r.t.): g = 2.103. EPR (solid, 77 K): g = 2.108. EPR (thf, 77 K): g_x = 2.013 (A_x = 1.8 mT), g_y = 2.045 (A_y = 4.2 mT), g_z = 2.182 (A_z = 16.4 mT).

α-[Cu(*p*-NO_2BP)$_3$trenNO_3]NO_3·(thf)$_{1.5}$(*i*Pr_2O)$_{0.25}$ (C4): A thf solution of (*p*-NO_2BP)$_3$tren (15.6 mg, 0.020 mmol, 1 mL) was added to a thf solution of $Cu(NO_3)_2$·$3H_2O$ (4.8 mg, 0.020 mmol, 1.0 mL). Slow vapour diffusion of diisopropyl ether at ambient temperature yielded yellow-green needles of **C4** (13.6 mg, 62%).

β-[(*p*-NO_2BP)$_3$trenNO_3]NO_3·(thf)$_{2.5}$ (C3): A thf solution of (*p*-NO_2BP)$_3$tren (78.0 mg, 0.10 mmol, 2.5 mL) was added to a thf solution of $Cu(NO_3)_2$·$3H_2O$ (25.3 mg, 0.105 mmol, 2.5 mL). Vapour diffusion of diethyl ether at ambient temperature to the resulting green solution yielded green needle-like crystals overnight. The crystals were filtered, washed with diethyl ether and dried in air to give **C3** (89.0 mg, 78%). Single crystals of **C3** were grown by adding an ice-cold thf solution of (*p*-NO_2BP)$_3$tren (15.6 mg, 0.020 mmol, 0.3 mL) to an ice-cold thf solution of $Cu(NO_3)_2$·$3H_2O$ (5.1 mg, 0.21 mmol, 0.3 mL) kept in an ice bath. Vapour diffusion of diethyl ether into this solution at temperatures of 5 °C (cold room) or –20 °C (freezer) yielded green needle-like crystals of **C3**. IR: $\tilde{\nu}$ = 3212 (w), 2864 (w br), 1598 (m), 1516 (s), 1500 (m), 1344 (s), 1282 (s) cm^{-1}. UV/Vis/NIR (reflectance): λ_{max} = 275, 330, 425, 695, 885 nm. UV/Vis/NIR (thf): λ_{max} (ε_{max}, $M^{-1}cm^{-1}$) = 400 (2940), 605 (230), 685 (270) nm. EPR (solid r.t.): g = 2.091. EPR (solid, 77 K): g = 2.098. EPR (thf, 77 K): g_x = 2.013 (A_x = 1.8 mT), g_y = 2.045 (A_y = 4.2 mT), g_z = 2.182 (A_z = 16.4 mT).

Crystal Data Collection and Reduction: The crystal was mounted in Paratone oil. Data were collected with a Bruker AXS APEXII diffractometer on Station 11.3.1[28] of the Advanced Light Source, Lawrence Berkeley National Laboratory, by using silicon monochromated radiation of wavelength λ = 0.77490 Å, at 150 K; the instrument was fitted with an Oxford Cryostream low-temperature attachment. The Bruker AXS APEX 2 software was used throughout the data collection and reduction.

Refinement

Compound C4: All non-hydrogen atoms were refined anisotropically except for the solvent molecules. All hydrogen atoms were placed geometrically except those on the secondary nitrogen atoms, these were found in the difference map and allowed to refine freely. Geometrical and displacement parameter restrains were used to model the solvent molecules. Displacement parameter restrains were used to model the nitro groups; even with these, the displacement parameter ratio max/min is around 5:1, a number of split site models were tried but did not refine well so they were left as they were.

Compound C3: The data were cut at 0.88 Å. All fully occupied non-hydrogen atoms and the major part of the disorder in the ligand

Table 4. Crystal data collection parameters for **C4** and **C3**.

Crystal	**C4**	**C3**
Empirical formula	$C_{52.50}H_{60.50}CuN_9O_{13.75}$	$C_{55}H_{65}CuN_9O_{14.50}$
M /g mol^{-1}	1101.14	1147.70
Crystal system	monoclinic	monoclinic
Space group	$P2_1/c$	$P2_1/n$
a /Å	22.1457(19)	12.516(1)
b /Å	9.1654(8)	29.989(2)
c /Å	27.201(2)	14.968(1)
α /°	90	90
β /°	103.222(2)	102.673(2)
γ /°	90	90
Volume /Å^3	5374.7(8)	5481.4(7)
Z	4	4
μ (Mo-K_α) /mm^{-1}	0.602	0.595
D_c /g cm^{-3}	1.361	1.391
No. data measured	47767	48388
Unique data (R_{int})	12315 (0.0550)	8425 (0.0724)
Observed data [I > 2(σ)I]	9149	6223
Final R_1[a], wR_2[b] (obs. Data)	0.0606, 0.1666	0.0551, 0.1411
Final R_1, wR_2 (all data)	0.0832, 0.1829	0.0796, 0.1573
ρ_{min},ρ_{max} /e Å^3	–0.922, 1.215	–0.458, 1.199

[a] $R = \Sigma(|F_o| - |F_c|)/ \Sigma|F_o|$. [b] $R' = [\Sigma w(|F_o| - |F_c|)^2/ \Sigma F_o^2]^{1/2}$, where $w = [\sigma^2(F_o)]^{-1}$.

were refined anisotropically. Hydrogen atoms were placed geometrically on the carbon atoms and refined with a riding model. The secondary amine hydrogen atoms were found in the difference map and allowed to refine freely. Geometrical and displacement parameter restrains were used in modelling the disorder in the ligand, the nitro groups and the solvent molecules. Even with these, the displacement parameter ratio max/min up to 5:1 was not ideal, which reflects the freedom of the ends of the ligand in the structure. Crystal data is summarized in Table 4.

CCDC-783563 and -783564 for **C4** and **C3**, respectively, contain the supplementary crystallographic data for this paper. These data can be obtained free of charge from The Cambridge Crystallographic Data Centre via www.ccdc.cam.ac.uk/datarequest/cif.

Acknowledgments

This work was supported by an Australia–Korea Foundation grant and the Australian Research Council through the Centre for Green Chemistry. The Advanced Light Source is supported by the Director, Office of Science, Office of Basic Energy Sciences, of the U.S. Department of Energy under Contract No. DE-AC02-05CH11231. A. A. acknowledges the award of a Monash Graduate Scholarship and a Monash International Postgraduate Research Scholarship.

[1] A. G. Blackman, *Polyhedron* **2005**, *24*, 1–39.
[2] N. Candelon, D. Lastecoueres, A. K. Diallo, J. R. Aranzaes, D. Astruc, J. M. Vincent, *Chem. Commun.* **2008**, 741–743; M. Schatz, M. Becker, O. Walter, G. Liehr, S. Schindler, *Inorg. Chim. Acta* **2001**, *324*, 173–179.
[3] J. L. Coyle, A. Fuller, V. McKee, J. Nelson, *Acta Crystallogr., Sect. C: Cryst. Struct. Commun.* **2006**, *62*, m472–m476.
[4] A. J. Fischmann, C. M. Forsyth, L. Spiccia, *Inorg. Chem.* **2008**, *47*, 10565–10574.
[5] J. Gazo, I. B. Bersuker, J. Garaj, M. Kabesova, J. Kohout, H. Langfelderova, M. Melnik, M. Serator, F. Valach, *Coord. Chem. Rev.* **1976**, *19*, 253–297.
[6] B. J. Hathaway in *Structure & Bonding, Vol. 57*, Springer, Berlin/Heidelberg, **1984**, pp. 55–118.
[7] K. Flinzner, A. F. Stassen, A. M. Mills, A. L. Spek, J. G. Haasnoot, J. Reedijk, *Eur. J. Inorg. Chem.* **2003**, 671–677; R. S. Glass, M. Sabahi, M. Hojjatie, G. S. Wilson, *Inorg. Chem.* **1987**, *26*, 2194–2196; S. F. Haddad, J. Pickardt, *Transition Met. Chem.* **1993**, *18*, 377–384; P. F. Kelly, A. M. Z. Slawin, K. W. Waring, *J. Chem. Soc., Dalton Trans.* **1997**, 2853–2854.
[8] G. A. van Albada, I. Mutikainen, U. Turpeinen, J. Reedijk, *J. Chem. Crystallogr.* **2007**, *37*, 489–496.
[9] A. Almesåker, P. Gamez, J. Reedijk, J. L. Scott, L. Spiccia, S. J. Teat, *Dalton Trans.* **2009**, 4077.
[10] Y. Akhriff, J. Server-Carrio, A. Sancho, J. Garcia-Lozano, E. Escriva, L. Soto, *Inorg. Chem.* **2001**, *40*, 6832–6840; B. J. Hathaway, *Coord. Chem. Rev.* **1983**, *52*, 87–169.
[11] G. Wilkinson, R. D. Gillard, J. A. McCleverty, *Comprehensive Coordination Chemistry: The Synthesis, Reactions, Properties & Applications of Coordination Compounds, Vol. 5*, 1st ed., Pergamon Press, Oxford, New York, **1987**.
[12] B. Lucchese, K. J. Humphreys, D. H. Lee, C. D. Incarvito, R. D. Sommer, A. L. Rheingold, K. D. Karlin, *Inorg. Chem.* **2004**, *43*, 5987–5998; N. Wei, N. N. Murthy, K. D. Karlin, *Inorg. Chem.* **1994**, *33*, 6093–6100.
[13] A. W. Addison, T. N. Rao, J. Reedijk, J. van Rijn, G. C. Verschoor, *J. Chem. Soc., Dalton Trans.* **1984**, 1349–1356.
[14] C. C. Addison, N. Logan, S. C. Wallwork, C. D. Garner, *Quarterly Rev.* **1971**, *25*, 289–322; G. J. Kleywegt, W. G. R. Wiesmeijer, G. J. Vandriel, W. L. Driessen, J. Reedijk, J. H. Noordik, *J. Chem. Soc., Dalton Trans.* **1985**, 2177–2184.
[15] A. J. Fischmann, A. C. Warden, J. Black, L. Spiccia, *Inorg. Chem.* **2004**, *43*, 6568–6578.
[16] K. Komiyama, H. Furutachi, S. Nagatomo, A. Hashimoto, H. Hayashi, S. Fujinami, M. Suzuki, T. Kitagawa, *Bull. Chem. Soc. Jpn.* **2004**, *77*, 59–72.
[17] F. Thaler, C. D. Hubbard, F. W. Heinemann, R. van Eldik, S. Schindler, I. Fabian, A. M. Dittler-Klingemann, F. E. Hahn, C. Orvig, *Inorg. Chem.* **1998**, *37*, 4022–4029.
[18] G. Golub, A. Lashaz, H. Cohen, P. Paoletti, A. Bencini, B. Valtancoli, D. Meyerstein, *Inorg. Chim. Acta* **1997**, *255*, 111–115.
[19] E. J. Laskowski, D. M. Duggan, D. N. Hendrickson, *Inorg. Chem.* **1975**, *14*, 2449–2459.
[20] W. Zhang, T. Jiang, S. M. Ren, Z. W. Zhang, H. S. Guan, J. S. Yu, *Carbohydr. Res.* **2004**, *339*, 2139–2143.
[21] M. Becker, F. W. Heinemann, S. Schindler, *Chem. Eur. J.* **1999**, *5*, 3124–3129.
[22] A. Bondi, *J. Phys. Chem.* **1964**, *68*, 441–451.
[23] H. D. Lutz, *J. Mol. Struct.* **2003**, *646*, 227–236; T. Steiner, *Angew. Chem. Int. Ed.* **2002**, *41*, 48–76.
[24] E. L. Muetterties, *Inorg. Chem.* **1965**, *4*, 769–771.
[25] P. Baran, M. Koman, D. Valigura, J. Mrozinski, *J. Chem. Soc., Dalton Trans.* **1991**, 1385–1390; M. Palaniandavar, R. J. Butcher, A. W. Addison, *Inorg. Chem.* **1996**, *35*, 467–471; G. A. van Albada, W. J. J. Smeets, A. L. Spek, J. Reedijk, *Inorg. Chim. Acta* **1999**, *288*, 220–225.
[26] A. Almesåker, J. L. Scott, L. Spiccia, C. R. Strauss, *Tetrahedron Lett.* **2009**, *50*, 1847–1850.
[27] F. Neese, *The Program EPR, a Modelling Approach*, University of Konstanz, Germany, **1993**.
[28] A. C. Thompson, H. A. Padmore, A. G. Oliver, S. J. Teat, R. S. Celestre, S. M. Clark, E. E. Domning, K. D. Franck, G. Y. Morrison, *AIP Conf. Proc.* **2004**, *705*, 482–485.

Received: July 30, 2010
Published Online: October 27, 2010

